

Preparation and bactericidal action of biofunctional polyacrylamide nanogels

Sadiya Anjum, Shamayita Patra, Bhuvanesh Gupta*

Bioengineering Laboratory, Department of Textile Technology, Indian Institute of Technology, New Delhi 110016, India

*Corresponding author, Tel: (+91) 11-26591416; E-mail: bgupta@textile.iitd.ernet.in

Received: 21 March 2016, Revised: 08 May 2016 and Accepted: 04 October 2016

DOI: 10.5185/amlett.2017.6562

www.vbripress.com/aml

Abstract

This study is aimed at the development of nanosilver embedded polyacrylamide (PAAm) bioactive nanogels and antimicrobial behavior of these functional nanogels. Nanogels were synthesized by polymerization of the monomer/silver nitrate as water phase in nanoemulsion using gamma irradiation process where radiation helps in the polymerization, nanogel crosslinking and the reduction of silver nitrate to nanosilver. Homogeneously dispersed nanosilver particles embedded within PAAm nanogel matrix having size in the range of 10-50 nm were achieved depending on the reaction conditions. Minimum inhibitory concentration and bacteriostatic efficacy of nanogels were investigated against bacterial strains of *Escherichia coli* and *Staphylococcus aureus*. The bioactive nanogels showed very effective antimicrobial behavior and showed mortality against both bacterial strains at very low concentration. The bactericidal action of functional silver nanoparticles against *Escherichia coli* was investigated by TEM analysis. It was observed that after treatment with bioactive nanogel, the cell wall of *Escherichia coli* was completely destroyed and punctured. Here, we propose that the bioactive nanogel by virtue of its hydrophilic and polar functionality is very much suitable for linking to different biomaterials for developing antimicrobial surfaces especially in surgical devices and synthetic implants. Copyright © 2016 VBRI Press.

Keywords: Polyacrylamide, nanogel, radiation, bacteria, minimum inhibitory concentration.

Introduction

The concept of using nanosilver particles for infection control has been the domain of significant interest to the biomedical and material scientists [1–3]. Silver nanoparticles are known to possess oligodynamic action for their behavior against antibiotic-resistant microbes, with low cytotoxicity towards mammalian cells [4]. In routine life, nanosilver is used for various medical applications, such as coatings in surgical devices, wound dressings, catheters, sutures, infusion systems and dental composites [5–9]. One of the problems associated with nanosilver technology is that it lacks the possibility of attaching to surface due to absence of any chemical functionality [10, 11]. The only way nanosilver may bind is by coordination to the sites on a surface. Therefore, an atmosphere of chemical functional groups around nanosilver particles would offer the possibilities of binding by hydrogen, ionic or by covalent interaction. That would mean that the nanosilver is confined within a nanogel of specific functionality.

Functional nanosilver may be achieved by creating an interactive polymer layer around the particles. This may be achieved by the silver reduction within a polymeric nanogel which would lead to the nanoparticles with functionality depending on the chemistry of the gel matrix. Such an approach would be entirely different

where nanosilver is prepared within another continuous matrix of gel. Various routes are available for the synthesis of nanocomposites containing silver nanoparticles either of the chemical, irradiation and physical methods. The chemical route involving fructose and herbal extracts have been recently used to develop nanosilver particles of various sizes [12,13]. Polyethylene glycol (PEG) on one hand helps in developing nanosilver particles [14]. On the other hand, terminal aldehyde groups are generated on the (PEG) chains which may provide site for crosslinking with amino groups of chitosan leading to a functional nanogel [15].

Radiation-induced synthesis has long been recognized as a suitable method for preparation of various gels and nanogels for biomedical applications [16–19]. The process offers easy control over designing specific physico-chemical characteristic of the nanoparticles. Radiation-induced synthesis of silver nanoparticles within hydrogel has been recently reported by our group, where gamma radiation was used for the simultaneous polymerization of methacrylic acid and the reduction of silver ions [16]. Chen et al. reported polyacrylamide stabilized silver nanoparticles through one-pot synthesis at higher temperature [17]. In another study, the radiation-induced synthesis of poly(vinylpyrrolidone) nanogels was carried out for drug delivery application with both inter and intra crosslinking of nanogels [18]. At the same time, the one-

step in situ preparation of silver nanoparticles in polymethyl methacrylate (PMMA) by radical polymerization has been employed to synthesize Ag/PMMA nanocomposites [19]. In the present work, we attempted radiation-induced synthesis of nanosilver encapsulated polyacrylamide (PAAm) nanogels as water-in-oil nanoemulsion. The concept is the silver be confined to the water phase along with the monomer in a water-in-oil nanoemulsion so that polymerization of the monomer and silver reduction proceed simultaneously within the nano confinement and produce a nanoparticle which has nanosilver embedded within the nanogel matrix. Therefore, our research efforts deal with the synthesis of nanosilver particles embedded into polymeric network with excellent antimicrobial activity and low cytotoxicity. The physical and biological characterization of bioactive nanogels has been investigated.

Experimental

Materials

Sodium bis (2-ethylhexyl) sulfosuccinate (AOT) was received from Fluka. Acryl amide (AAM), ethyl methyl ketone (EMK), heptane, silver nitrate, glutaraldehyde, ethanol and sodium chloride (NaCl) were supplied by Merck India. Luria broth and agar-agar, were obtained from Hi Media Laboratories, India. Bacterial strains of *Escherichia coli* (*E. coli*) and *Staphylococcus aureus* (*S. aureus*) were provided by IIT Delhi. Ultra-pure water with resistivity less than 18 MΩcm produced by a Millipore Milli-Q system was used in all experiments. ⁶⁰Co gamma radiation source of 800 curies (dose rate of 0.16 kGy/h), supplied by Bhabha Atomic Research Centre, India, was used for the irradiation of the samples.

Preparation of nanogel

Nanoemulsion polymerization was used to prepare nanogels in water-in-oil system as per the process reported earlier [16]. Water phase was prepared by dissolving silver nitrate and AAm (monomer) in Milli-Q water. AOT was added as the surfactant in heptane. The water phase [AAM: AgNO₃] was mixed in oil phase [AOT: heptane] and the whole mixture was then placed on constant stirring for 10 min. The solution was transferred to reaction tube, deaerated by bubbling nitrogen for 15 min and was sealed. The nanoemulsion was subjected to polymerization using γ -radiation for different timings. After the completion of reaction, the nanoemulsion was destabilized by the addition of sodium chloride so that the nanoparticles settled down. The precipitate was washed repeatedly with ethyl methyl ketone (EMK) to remove AOT. The remaining precipitate (nanoparticles) was repeatedly washed with EMK, and dried under vacuum.

Energy dispersive X-ray microanalysis (EDX)

The presence of silver in nanogel samples was monitored by EDX analysis. The sample was placed on an aluminum sample stub and coated with carbon using Auto-Fine Coater JFC-1600 (Joel, USA). The images and the silver

content of the samples were obtained with RONTEC's EDX Model QuanTax 200 (SDD technology, USA).

Ultraviolet visible (UV-vis) spectroscopy

The formation of silver nanoparticles in the colloidal solution was monitored using a Perkin Elmer Lambda 35 UV-Vis spectrophotometer at the wavelength range of 200 to 600 nm. The plasmon resonance band characteristic of monodispersed nanoparticles appeared at ~ 420 nm was monitored. Color changes in the colloidal solution were monitored by visual inspection. Digital images of the samples were captured with a digital still camera (Cannon-550D) at an optical zoom of 4X.

High resolution transmission electron microscopy (HRTEM)

The morphology of nanogel particles was observed under a TECNAI TEM (Fei, Electron Optics) TEM, operated at 200 kV and equipped with Olympus Soft Imaging Solutions GmbH (software: iTEM; TEM Camera: Morada 4008 × 2672 pixel max) recording system. The samples were prepared by placing one drop of the aqueous nanogel on a carbon-coated copper TEM grid and dried at room temperature. Particle size distribution was derived from a histogram considering more than 50 particles measured using multiple TEM micrographs.

Determination of minimum inhibitory concentration (MIC)

The minimum inhibitory concentration (MIC) of bioactive nanogels was determined by batch cultures containing varying concentration of bioactive nanogels in suspension (0.1, 0.25 and 0.5 mg/mL) [20]. Varying concentration of bioactive nanogels was added in 100 mL nutrient broth solution in flasks. Solutions were sonicated for 30 min at room temperature prevent aggregation of the nanogel particles. Subsequently, 500 μ L of the freshly prepared bacterial suspension were inoculated in flask in order to maintain initial bacterial concentration 10⁵–10⁶ CFU/mL. Solutions were incubated in an orbital shaker at 250 rpm and 37°C. Bacterial growths was measured as change in absorbance at 600 nm by using a spectrophotometer (Perkin Elmer Lambda 35 UV-vis spectrophotometer). The experiment also included a positive control (containing bioactive nanogels in broth, without bacterial inoculum) and a negative control (containing bacterial inoculum in broth, without bioactive nanogels). The negative control indicated the microbial growth profile in the absence of nanoparticles. The absorbance values for positive controls were subtracted from the experimental values (containing varying concentration of nanogels in broth and bacterial inoculum). All the experiments were carried out in triplicate measurements.

Antimicrobial studies

Antibacterial studies of nanogels were carried out by colony count method, according to test method AATCC 100-1998 [16]. The antibacterial efficiency of nanogel was monitored against gram negative bacteria,

Escherichia coli (*E. coli*) and gram positive *Staphylococcus aureus* (*S. aureus*). Bacterial colonies were obtained from an overnight culture suspended in Luria Broth and the turbidity was adjusted to 0.5 McFarland standards. The samples (~20 mg) were placed in contact with 6 mL bacterial suspension in Luria Broth having 10^6 CFU mL⁻¹. All suspensions were vortexed and incubated at 37°C for 24 h. The colonies were counted by the spread plate method. The inoculum (200 μ L) was uniformly spread on nutrient agar plates which were incubated at 37°C and the colonies were counted after 24 h. All experiments were conducted under sterile conditions.

Bactericidal action of nanogel

Bactericidal action of nanogel was observed by high resolution transmission electron microscope (TECNAI TEM (Fei, Electron Optics). Nanogel was inoculated in bacterial suspension in Luria broth and fixed by 2.5% glutaraldehyde solution for 24 h. Sample was cultured for 24 h overnight incubation at 37°C, 95% air/5% CO₂. Excess glutaraldehyde was removed by three gentle rinses with ultrapure water and then re-suspended in sterilized ultrapure water. For TEM analysis, the samples were prepared by placing one drop of the suspension solution on a carbon-coated copper TEM grid and dried at room temperature.

Results and discussion

The bioactive nanogels were prepared by polymerization of acrylamide in water-in-oil nanoemulsion system and the influence of various parameters on the nanoparticle formation was investigated. The schematic representation of the radiation induced nanogel formation is presented in **Fig. 1**. The nanogel network of polyacrylamide was obtained by γ -irradiation which takes into account the polymerization of the acrylamide monomer, crosslinking of polyacrylamide chains and the reduction of silver ions, simultaneously.

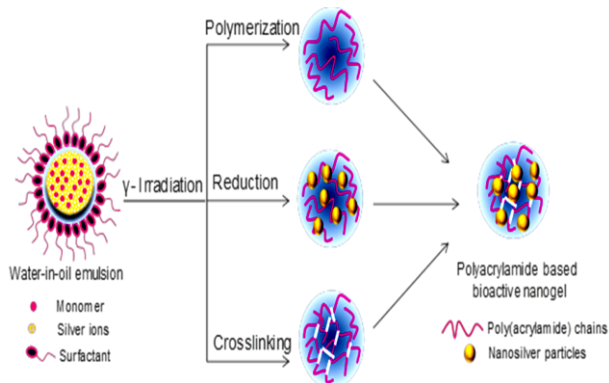


Fig. 1. Schematic representation of the development of polyacrylamide nanosilver bioactive nanogels.

The elemental analysis of nanogel sample was carried by EDX and is presented in **Fig. 2**. The EDX spectrum shows a distinctive energy peak at around 0.2 keV, characteristic of carbon and oxygen along with a peak at 0.39 KeV, which confirms the presence of nitrogen in

nanogel due to amide functionality (**Fig. 2a**). However, in nanosilver embedded nanogel another strong peak appears at ~3 keV, which shows the presence of elemental silver within the nanogel matrix (**Fig. 2b**). The EDX pattern of Ag, O and C was found to be with 37.2, 36.7 and 19.1% respectively. The nanogel formation has been found to be significantly affected by the reaction conditions, such as irradiation time, water phase, and AOT concentration. A systematic evaluation of these parameters is presented in the subsequent sections.

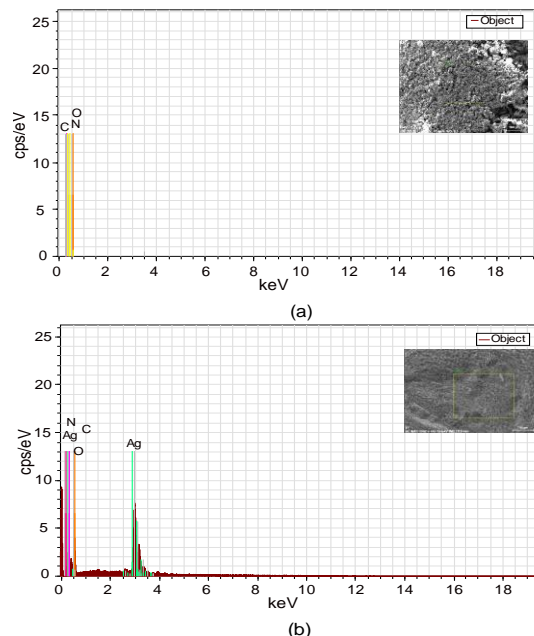


Fig. 2. EDX studies with TEM image of the (a) pure PAAm gel (b) bioactive nanogel particles. Reaction conditions: oil phase, heptane; AOT, 8%; water phase, 2% [AAM, 5.6×10^{-2} mol/L; AgNO₃, 2.3×10^{-2} mol/L]; radiation time, 120 min.

Fig. 3 shows the UV-vis absorption spectra of nanogels prepared at 10 min to 12 h of irradiation time. UV-vis absorption measurements provides a deeper insight into the optical properties of the nanoparticles preparation, confirming the growth of nanoconfined silver particles and the relative size distribution and surface properties of nanogels.

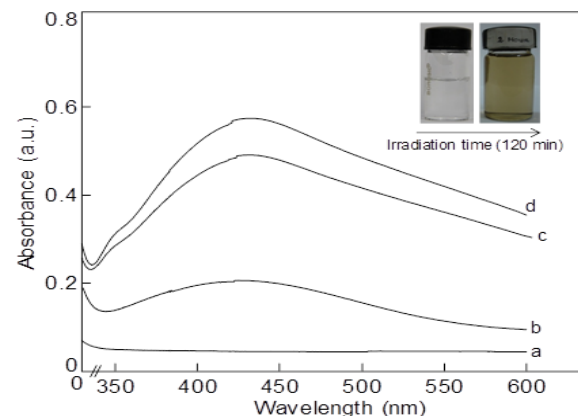


Fig. 3. UV-visible studies of bioactive nanogels with the radiation time (a) 0 min, (b) 10 min, (c) 120 min and (d) 12 h. Reaction conditions: oil phase, heptane; AOT, 8%; water phase, 2% [AAM, 5.6×10^{-2} mol/L; AgNO₃, 2.3×10^{-2} mol/L].

Silver salt reduction was monitored visually since the colorless salt solution changed to a deep brown color (Inset in Fig. 3) after 2 h irradiation. The characteristic plasmon band ranging between 410 and 460 nm, appeared within 10 min of the radiation-induced reduction process. Certainly, the intensity variation is due to the difference in the size of the synthesized nanoparticles. Beyond irradiation time of 120 min, there was no appreciable change in the intensity of the plasmon resonance band of nanosilver particles at 420 nm, indicating the completion of reduction process within 120 min.

The TEM images of the nanogels with particle size distribution are presented at various irradiation durations are presented in Fig. 4.

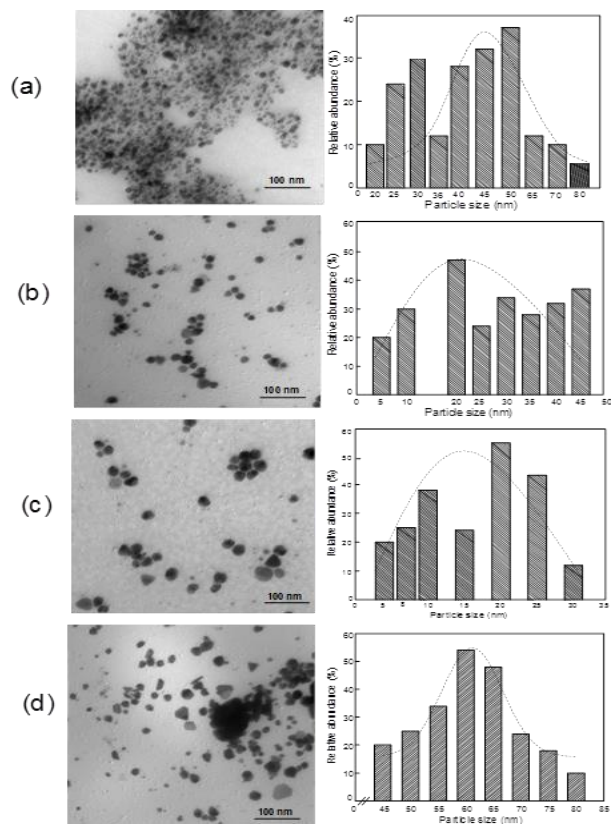


Fig. 4. TEM images and particle size distribution of the bioactive nanogel particles with the radiation time (a) 10 min, (b) 30 min, (c) 120 min and (d) 12 h. Reaction conditions: oil phase, heptane; AOT, 8%; water phase, 2% [AAm, 5.6×10^{-2} mol/L; AgNO_3 , 2.3×10^{-2} mol/L].

During the nanogel formation, the reduction of Ag^+ to Ag^0 was accomplished by the radiation where polyacrylamide moiety provides stabilizing effect to the nanosilver. The functional nanosilver particles exhibited a spherical shape and are evenly dispersed in polyacrylamide chains. The nanoparticles retain spherical shape and slightly agglomerated into the gel for the initial 10 min of irradiation time (Fig. 4a). After 30 min, regular spherical shape and well dispersed particles with average size in the range of 5-50 nm were observed. At irradiation time of 120 min, the majority of particles were confined to 5-30 nm size which is an indication for sufficient homogeneity and proper dispersion of nanoparticles. However, the particle size became larger and a bit agglomerated when the irradiation was time increased to

12 h (Fig. 4d). Highly dense nanogel networks and less individual particles tend to appear. Here, the irradiation plays a very interesting role. Initial irradiation leads to the gradual polymerization and crosslinking of the polyacrylamide nanogel. As the irradiation proceeds further as higher for 12 h, the nanogel particles themselves tend to crosslink together and appear as the agglomerated particles. Under such a scenario, it seems that the reaction time of 120 min is most optimum where the particles are uniformly spherical in shape and are well dispersed in the gel matrix.

The size of the nanogel particles is strongly influenced by the variation in water phase (Fig. 5). The higher water phase involves high monomer content which eventually leads to the formation of bigger micelle size and hence the larger particle size. As the water phase increased from 1 to 3%, the size of nanosilver particles was found to be in the range of 10–80 nm. Spherical nanosilver particles were found to be dispersed homogeneously in all samples. Monodispersed particles were observed in 2% water phase and were considered as the optimized water phase for nanogel preparation. With increasing AOT concentration, the particle size showed decreasing trend in the size has been shown in Fig. S1. At 8% AOT concentration, the emulsion was stable and well dispersed nanoparticles of 20 nm were observed. Therefore, 8% AOT concentration has been optimized for the growth of monodispersed particles of nanogels.

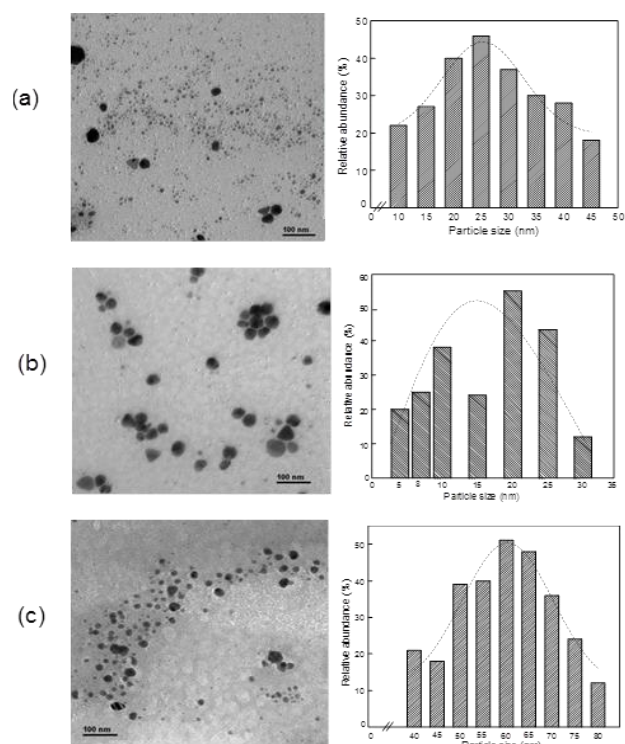


Fig. 5. TEM images of the and particle size distribution bioactive nanogel particles with the varying water phases (a) 1% w/o, (b) 2% w/o and (c) 3% w/o. Reaction conditions: oil phase, heptane; AOT, 8% [AAm, 5.6×10^{-2} mol/L; AgNO_3 , 2.3×10^{-2} mol/L]; radiation time, 120 min.

The MIC values of bioactive nanogels against both type of bacterial strains was investigated. The growth profiles of microbial strains in the presence of varying

concentration of nanogels (0.1, 0.25 and 0.5 mg/mL) are shown in **Fig. 6A**. As the concentration of nanogels in suspension was increased from 0.1 mg/mL to 0.5 mg/mL, the growth profile of microbes decreased by lowering the value of maximum absorbance (at 600 nm). Similar trend was obtained against both types of bacterial strains. Initial bacterial inoculate concentration was kept constant at 10^5 – 10^6 CFU/mL irrespective of nanogel concentration. As concentration of nanogels increased upto 0.5 mg/mL there was no bacterial growth was observed in the broth media against both microbial strains. It may therefore be concluded that 0.5 mg/mL is the MIC values of bioactive nanogels against both type of bacterial strains.

The antibacterial efficacy of nanogels was evaluated against *E. coli* and *S. aureus* by colony formation method (**Fig. 6B**). As we concluded from MIC results, 0.5 mg/mL (500 ppm) of bioactive nanogels is sufficient for complete bacterial growth against both classes of bacteria. Therefore, 0.5 mg/mL was used for this study and it is seen that the nanogel has high antibacterial activity as evidenced by complete inhibition of the bacterial growth. This suggests a highly efficient bioactive system which may impede any microbial infection caused by *E. coli* and *S. aureus*.

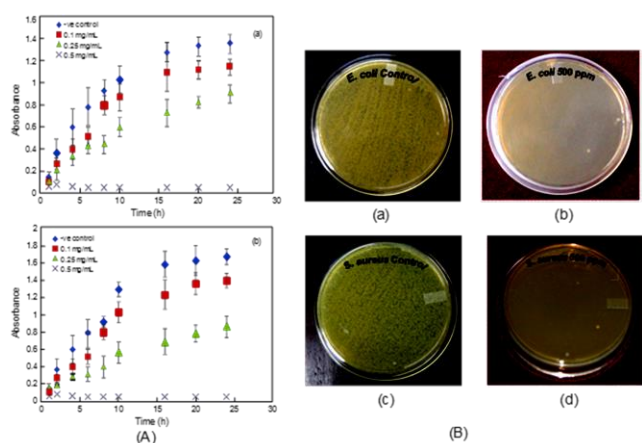


Fig. 6. (A) Growth profile of bioactive nanogel with varying concentrations against (a) *E. coli* and (b) *S. aureus*. (B) Colony formation images of bioactive nanogel against *E. coli* (a), (b) and *S. aureus* (c) and (d).

A more visible scenario of the bactericidal nature of bioactive nanogels is evident from the TEM images shown in **Fig. 7**. **Fig. 7 a** and **b**, represents the TEM images of live *E. coli* without any treatment with nanogels appeared as normal with their characteristic shape. While other figures (**Fig. 7c-f**) present different stages of killing phenomena of *E. coli* by nanogel particles and homogeneous distribution nanogel particles in *E. coli*. Bacterial cell wall can make up an effective barrier against nanosilver but nanosilver particles take multidirectional approaches to kill bacteria with high efficiency due to their small size. The bactericidal action of the nanosilver particles was observed by analyzing the structural morphology and growth of *E. coli*. **Fig. 7c** represents the bioactive nanogel treated *E. coli* and exhibited appreciable shrinkage with irregular shape and outer membrane was disintegrated. The TEM micrograph

in **Fig. 7 d** and **e**, showed that nanogels were present on the cell membrane and they appeared to be attached to the lipopolysaccharide layer present in the cell wall of *E. coli*.

Fig. 7f represents the TEM image of punctured or dead *E. coli* after treatment with functional silver nanoparticle. In bacterial cell, metabolic activity involves the mechanism of obtaining energy to perform all the biological processes. It was found that nanosilver particles are likely to disturb all functions in bacteria. Nano silver particles sized less than 10 nm, accumulate within the cell membrane through electrostatic attraction and ultimately lead to the cell death. The nanoparticles are able to penetrate cytoplasm where they disturb cell metabolism and other biological functions. Disfunctioning of the cell wall may also be associated with catalytic behavior of nanosilver, Ag is converted to Ag^+ on contact with the hydrophilic cytoplasm. The resulting Ag^+ ions interact with the thiol groups of enzymes that are necessary for bacterial respiration and this leads to the cell death. Also, positively charged Ag^+ ions can link with the negatively charged bacterial cell wall leading to the disintegration of cell membrane and leakage of the cell constituents. Alternatively, Ag^+ may also interfere with DNA replication resulting in bacterial inhibition [21,22].

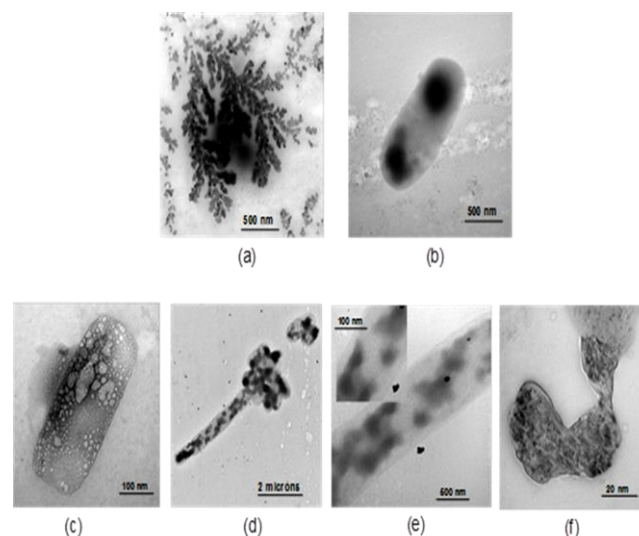


Fig. 7. Bactericidal action of bioactive nanogel against *E. coli*, TEM image of (a) and (b) untreated *E. coli*, (c) denatured *E. coli* (d) and (e) nanogel interaction with *E. coli*, (f) punctured *E. coli*. Nanogel content, 500 ppm (0.5 mg/mL).

Our study is very much supported by the observation for the interaction between silver ions and respiratory chain enzymes in *E. coli*. It was found that the silver ions bind to functional groups of amino acids making up enzymes and that activity inhibits the efficient electron transport via the respiratory chain [23]. After the treatment, a sharp increase in the leakage of saccharides and proteins in bacterial cells was observed leading to deformation and fragmentation.

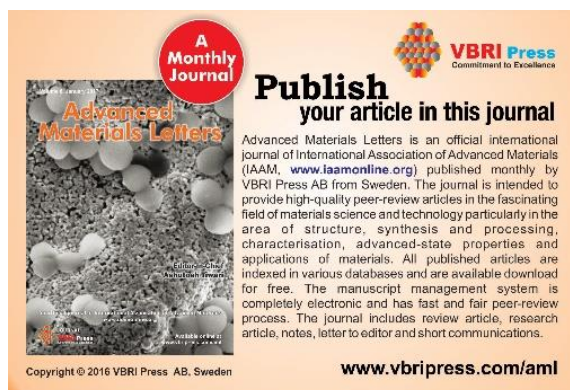
Conclusion

Our aim of this work has been to develop an approach for the development of functional nanosilver particle which may interact with a wide variety of the material surface.

This has been achieved by in-situ generation of nanosilver particle while polymerization of acrylamide takes place simultaneously. Since nanosilver is embedded within a hydrogel nanoparticle, the whole nanoparticles not only become bioactive but also acquire polar functionality of amide groups which would allow it to interact with any biomaterial surface by hydrogen bonding or by polar interaction. These nanogels have been synthesized by nanoemulsion polymerization using gamma irradiation process which performs three simultaneous functions, *i.e.* polymerization of acrylamide, crosslinking of polyacrylamide chains and reduction of silver ions. Well dispersed nanosilver particles within PAAm gel matrix in the size range of 10-50 nm are produced. The MIC value of bioactive nanogel is 0.5 mg/mL and showed highly effective antimicrobial behavior, mortality against *E. coli* and *S. aureus*. TEM images show the effective bactericidal performance of these nanogels against *E. coli*. The functional nanogels leads to complete check on completely destroy the cell wall of *E. coli*. This study offers an attractive nanogel material which is effective for infection control. The beauty of this bioactive nanogel is that the nanosilver is embedded within the nanogel matrix.

References

- Mahmoudi, M.; Serpooshan, V. *ACS Nano*. **2012**, *6*, 2656.
DOI: [10.1021/nn300042m](https://doi.org/10.1021/nn300042m).
- Kumar, A.; Vemula, P.K.; Ajayan, P.M.; John, G. *Nat. Mater.* **2008**, *7*, 236.
DOI: [10.1038/nmat2099](https://doi.org/10.1038/nmat2099).
- Morones, J.R.; Elechiguerra, J.L.; Camacho, A.; Holt, K.; Kouri, J.B.; Ramirez, J.T.; Yacaman, M.J. *Nanotechnology*. **2005**, *16*, 2346.
DOI: [10.1088/0957-4484/16/10/059](https://doi.org/10.1088/0957-4484/16/10/059).
- Gaillet, S.; Rouanet, J.M. *Food Chem. Toxicol.* **2015**, *77*, 58.
DOI: [10.1016/j.fct.2014.12.019](https://doi.org/10.1016/j.fct.2014.12.019).
- Nair, L.S.; Laurencin, C.T. *J. Biomed. Nanotech.* **2007**, *3*, 301.
DOI: [org/10.1166/jbn.2007.041](https://doi.org/10.1166/jbn.2007.041).
- Mijnendonckx, K.; Leys, N.; Mahillon, J.; Silver, S.; Van Houdt, R. *Biomaterials*. **2013**, *26*, 609.
DOI: [10.1007/s10534-013-9645-z](https://doi.org/10.1007/s10534-013-9645-z).
- Seltenrich, N. Nanosilver: weighing the risks and benefits. *Environ. Health Perspect.* **2013**, *121*, 220.
DOI: [10.1289/ehp.121-a220](https://doi.org/10.1289/ehp.121-a220).
- Wei, L.; Lu, J.; Xu, H.; Patel, A.; Chen, Z.S.; Chen, G. *Drug Discov. Today*. **2015**, *20*, 595.
DOI: [10.1016/j.drudis.2014.11.014](https://doi.org/10.1016/j.drudis.2014.11.014).
- Olga, D.; Hendrickson, S.G.; Klochkov, O.V.; Novikova, I.M.; Bravova, E.F.; Shevtsova, I.V.; Safenkova AV, Zherdev SO, Bachurin BB. *Toxicol. Lett.* **2016**, *241*, 184.
DOI: [10.1016/j.toxlet.2015.11.018](https://doi.org/10.1016/j.toxlet.2015.11.018).
- Li, X.; Lenhart, J.J. *Environ. Sci. Technol.* **2012**, *46*, 5378.
DOI: [10.1021/es204531y](https://doi.org/10.1021/es204531y).
- Shekhar, A.; Soumyo, M.; Suparna, M. *Nanoscale*. **2013**, *5*, 7328.
DOI: [10.1039/c3nr00024a](https://doi.org/10.1039/c3nr00024a).
- Anjum, S.; Sharma, A.; Tummalapalli, M.; Joy, J.; Bhan, S.; Gupta, B. *Int. J. Polym. Mater. Polym. Biomater.* **2015**, *64*, 894.
DOI: [10.1080/00914037.2015.1030660](https://doi.org/10.1080/00914037.2015.1030660).
- Anjum, S.; Gupta, A.; Sharma, D.; Gautam, D.; Bhan, S.; Sharma, A.; Kapil, A.; Gupta, B. *Mat. Sci. Eng. C*. **2016**, *64*, 157.
DOI: [10.1016/j.msec.2016.03.069](https://doi.org/10.1016/j.msec.2016.03.069).
- Luo, C.; Zhang, Y.; Zeng, X.; Zeng, Y.; Wang, Y. *J. Coll. Interf. Sci.* **2005**, *288*, 444.
DOI: [10.1016/j.jcis.2005.03.005](https://doi.org/10.1016/j.jcis.2005.03.005).
- Krishna Rao, K.S.V.; Palem, R.R.; Yong-III, L. *Carbo. Polym.* **2012**, *87*, 920.
DOI: [10.1016/j.carbpol.2011.07.028](https://doi.org/10.1016/j.carbpol.2011.07.028).
- Gupta, B.; Gautam, D.; Anjum, S.; Saxena, S.; Kapil, *Rad. Phys. Chem.* **2013**, *92*, 54.
DOI: [org/10.1016/j.radphyschem.2013.07.020](https://doi.org/10.1016/j.radphyschem.2013.07.020).
- Meng, C.; Li, Y.W.; Jian, T.H.; Jun, Y.Z.; Zh, Y.L.; Dong, J.Q. *J. Phys. Chem. B*. **2006**, *110*, 11224.
DOI: [10.1021/jp061134n](https://doi.org/10.1021/jp061134n).
- Jung, C.A.; Alia, W.; Byungnam, K.; Aaron, B.; Dianne, P.; Wyatt, N.V.; Joseph, S.; Mohamad, A.S. Radiation-induced synthesis of poly(vinylpyrrolidone) nanogel. *Polymer*. **2011**, *52*, 5746.
DOI: [10.1016/j.polymer.2011.09.056](https://doi.org/10.1016/j.polymer.2011.09.056).
- Singh, N.; Khanna, P.K. In situ synthesis of silver nano-particles in poly(methylmethacrylate). *Mater. Chem. Phys.* **2007**, *104*, 367.
DOI: [10.1016/j.matchemphys.2007.03.026](https://doi.org/10.1016/j.matchemphys.2007.03.026).
- Agnihotri, S.; Mukherji, S.; Mukherji, S. Size-controlled silver nanoparticles synthesized over the range 5–100 nm using the same protocol and their antibacterial efficacy. *RSC Adv.* **2014**, *4*, 3974.
DOI: [10.1039/c3ra44507k](https://doi.org/10.1039/c3ra44507k).
- Holt, K.B. Bard, A.J. *Biochemistry*. **2005**, *44*, 13214.
DOI: [10.1021/bi050854z](https://doi.org/10.1021/bi050854z).
- Sondi, I.; Salopek, S.B. *J. Coll. Interf. Sci.* **2004**, *275*, 177.
DOI: [10.1016/j.jcis.2004.02.012](https://doi.org/10.1016/j.jcis.2004.02.012).
- Danielle, M.; Pares, C.R.; Hongtao, Y. *J. Food Drug Anal.* **2014**, *22*, 116.
DOI: [10.1016/j.jfda.2014.01.010](https://doi.org/10.1016/j.jfda.2014.01.010).



A Monthly Journal

Advanced Materials Letters

Publish your article in this journal

Advanced Materials Letters is an official international journal of International Association of Advanced Materials (IAAM, www.iaamonline.org) published monthly by VBRI Press AB from Sweden. The journal is intended to provide high-quality peer-review articles in the fascinating field of materials science and technology particularly in the area of structure, synthesis and processing, characterisation, advanced-state properties and applications of materials. All published articles are indexed in various databases and are available download for free. The manuscript management system is completely electronic and has fast and fair peer-review process. The journal includes review article, research article, notes, letter to editor and short communications.

Copyright © 2016 VBRI Press AB, Sweden

www.vbripress.com/aml